communications earth & environment

Article

https://doi.org/10.1038/s43247-024-01369-9

Large spread in marine heatwave assessments for Asia and the Indo-Pacific between sea-surface-temperature products

Xuewei Zhang [1,2], Ning Zhao [3] ✉, Zhen Han [2] ✉ & Zhijun Dai[1]

Prolonged extremely warm ocean temperatures have great impacts on both natural ecosystems and human communities. These phenomena (i.e., marine heatwaves) could be easily monitored globally by satellite-based sea surface temperatures; however, the choice of datasets may lead to potential uncertainties in the marine heatwave assessment. Here we compared the marine heatwaves using three commonly used satellite products to illustrate the uncertainties over Asia and the Indo-Pacific. Distinct differences were found in the occurrence, duration, and long-term trend of marine heatwaves over both coastal and open oceans, while some discrepancies could become comparable with the obtained metrics themselves. Although differences in mean sea surface temperatures or their variances among datasets could not explain the abovementioned discrepancies, different sensors, procedures, and sea ice treatments in each dataset may contribute partially. Overall, our study suggests that the use of multiple datasets is crucial for evaluations of extreme events.

Prolonged extremely warm ocean temperatures, namely marine heatwaves (MHWs), are proven to have a great impact on the marine ecosystem, the atmosphere aloft, and human communities[1–5]. Generally, MHWs could be identified by discrete prolonged warm events with the ocean temperature (mostly, the sea surface temperature, SST) anomalies above a certain threshold[6]. Based on that, recent studies suggest that MHWs are becoming longer and more frequent all over the world[7–9], while more long-lasting MHWs have been observed[10–12]. Particularly, from 1925 to 2016, the global increase in MHW frequency and duration led to 54% more MHW days[13]. More recently, it is also found that coastal MHW occurrence and duration increased by about 1−2 events per decade and 5−10 days per decade globally during the past 25 years, respectively[14]. Some studies further suggest that the globally averaged MHW days may become over 112 days per year by the end of the twenty-first century under current carbon emissions, and the most severe MHWs that occur once every hundreds of years may become annual events[7].

The enhancement of MWHs has been observed globally; however, they did not increase homogeneously due to their various drivers[8,13–15], including SST warming[16,17], climate variations[18,19], and ocean dynamics[20,21], leading to challenges in predicting/projecting their future changes[22,23]. It is found that the warming of mean SST acts as the main driver of increasing MHWs[16], which also has a certain impact on the SST variance and further enhances MHW occurrence[18]. Global and regional scale climate changes, such as the El Niño–Southern Oscillation (ENSO) and the Pacific Decadal Oscillation, greatly modulate MHW characteristics via their impacts on the surface heating (by influencing the pressure system and hence the cloud cover) and air-sea interactions (e.g., wind-current responses and mixed layer processes[14,19,24]). In addition to that, oceanic phenomena, like the western boundary currents[15,25] and coastal upwellings[26], could influence MHWs via heat transport. Moreover, these drivers may act coherently, resulting in complex responses of MHWs in some specific regions, such as Asia and the Indo-Pacific (AIP) region[20,27].

On the other hand, as more and more studies focused on MHWs and their variabilities, a few studies noticed that the detected MHWs strongly depend on the selected dataset[6,8,14]. Particularly, a recent study was conducted using multi-product-based analysis for coastal MHWs and showed a large variety in both magnitude and trend among the results using different satellite-based SSTs[14]. Although some studies suggest the spatial

[1]State Key Laboratory of Estuarine and Coastal Research, East China Normal University, Shanghai 200062, China. [2]College of Oceanography and Ecological Science, Shanghai Ocean University, Shanghai 201306, China. [3]Center for Coupled Ocean-Atmosphere Research, Research Institute for Global Change, Japan Agency for Marine-Earth Science and Technology, Yokosuka 2370061, Japan. ✉e-mail: zhaoning@jamstec.go.jp; zhhan@shou.edu.cn

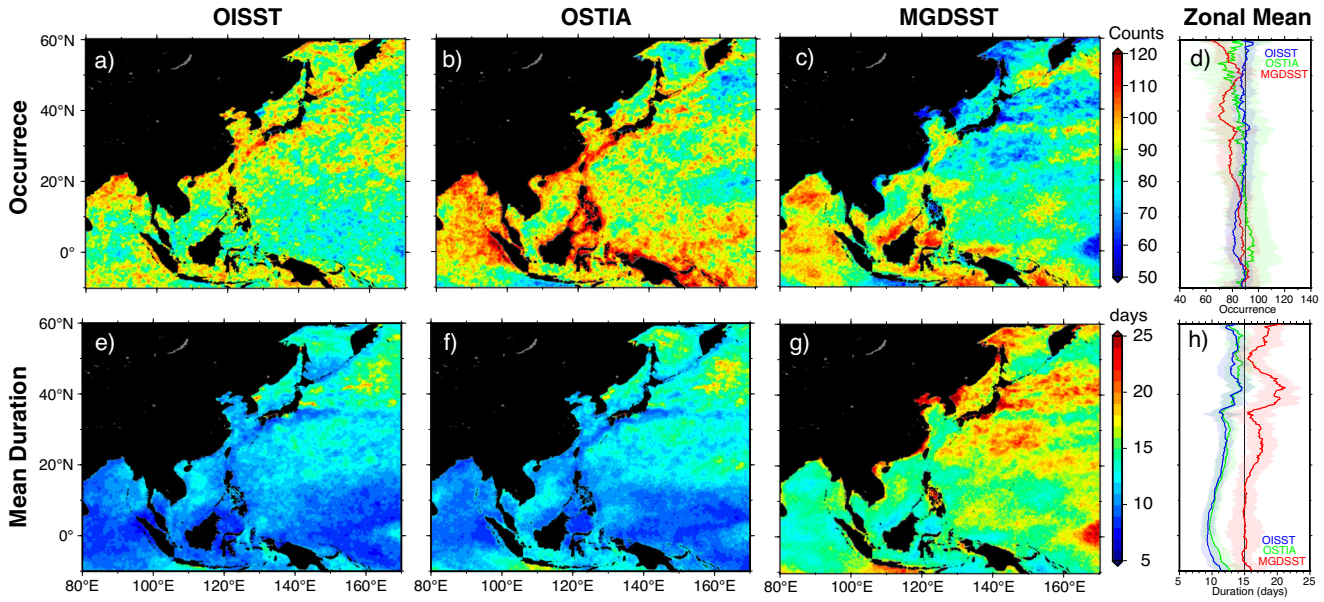

Fig. 1 | Metrics of MHWs based on OISST, OSTIA, and MGDSST. a–**c** Total occurrence and (**e**–**g**) the mean durations of marine heat waves (MHWs). Their zonal means are shown in (**d**, **h**) (solid lines), and the shading represents their standard deviations.

distributions and the time series of MHWs using different SST datasets were generally similar[13], the spread was actually large from a regional perspective (see Fig. S4 in ref. 13). One possible reason is that recent SST products do have similar mean states and variabilities, making them all acceptable in climate studies[28]. However, as shown in the studies mentioned above, it may not be true for evaluating MHWs.

Among the hotspots of MHWs, the AIP region is of particular interest, as it is dominated by complex climate and oceanic variations. With the world's largest population and abundant marine biodiversity, including the large area of coral reefs and related marine ecosystems, the AIP region is also one of the most vulnerable regions to MHWs[29–31]. Recent studies also demonstrated that the AIP region has warmed faster than the global mean in the last four decades[32–35], which induced the increase in MHW activity. Such enhancement was observed in the entire AIP region from the tropics to mid-latitudes[27,36–38]. Nevertheless, most previous studies were conducted based on only one dataset, leading to potential uncertainties in our current assessments of MHWs over this region.

Therefore, in this study, our primary goal is to estimate the general characteristics of MHWs over the AIP region and provide quantitative analyses of the potential uncertainties when using different datasets. Further interest is also given to whether the discrepancies have certain patterns or sources, which may help us reduce them. To do so, we compared MHWs obtained by three commonly used SST datasets, including the Optimum Interpolation Sea Surface Temperature (OISSTv2.1[39,40]), the Operational Sea Surface Temperature and Ice Analysis (OSTIA[41]) system, and the Merged satellite and in situ data Global Daily Sea Surface Temperature (MGDSST[42]), which are proved to have low biases compared to in situ data[28,43]. Moreover, since the reference depths of each SST dataset are not identical, we focused on the occurrence and related durations, which are sufficient to represent the likelihood of the estimated MHWs. Based on our analyses, while all three datasets show some similar patterns, large uncertainties (defined by the ratios between the variance of metric differences and the variance of the baseline from OISST) were seen in their occurrence, durations, and long-term trends. These discrepancies were not related to the mean SSTs or their variances in different datasets; however, the configurations in each SST analysis may contribute partially. Globally extended works are also conducted, suggesting such discrepancies are common in all the oceans (see Supplementary Figs. 8 and 9).

Results and discussion

General Conditions of MHWs

Figure 1 shows the occurrences and mean durations of MHWs over the AIP region based on three SST datasets: OISST, OSTIA, and MGDSST. In general, during the last four decades, MHWs tend to be found near the coast and the regions dominated by warm currents, such as the Kuroshio and its extension region. Results also show that some MHW-rich areas were connected and covered large regions of the marginal seas and the Maritime Continent (MC), suggesting those MHW events may not have occurred individually but were highly organized. On the other hand, more frequent MHWs were often accompanied by shorter durations (Fig. 1e-g; also see Supplementary Fig. 1 for the relations between occurrence and durations).

It is found that MHWs last about 10–15 days in most regions, while only some specific regions suffered from MHWs with durations longer than 20 days, such as the eastern coast of the northern Korean Peninsula, the Oyashio region, and the western subarctic gyre region (the northeast corner of our domain). In addition, unlike the occurrence, durations of MHWs exhibited a weak but clear dependence on the latitude, which is longer in the north and shorter in the south (Fig. 1h).

Although we obtained some similar patterns of MHWs based on the three SST datasets, great differences among them could not be ignored. In the tropical regions, much fewer MHWs were detected by OISST (Fig. 1a, d), while the numbers could become almost 50% larger if we used OSTIA (see Supplementary Fig. 2). Compared to them, although MGDSST showed moderate numbers of MHWs, it showed more MHWs over the offshore regions away from coastlines, such as the central Bay of Bengal (BOB) and the areas northwest of Kalimantan Island. However, situations changed in higher latitudes. In the regions north of 20°N, OISST had the highest occurrence among the three datasets, while much fewer MHWs were found in MGDSST, especially near 40°N (Fig. 1d).

Interestingly, although the occurrence of MHWs showed large differences between OSTIA and OISST, they had similar mean durations in most regions with differences of no more than 3 days (Fig. 1e, f), except in the MC, the central North Pacific, and the Sea of Okhotsk (OS; Fig. 1d, f; also see Supplementary Fig. 2). Unlike the small differences between OISST and OSTIA, MHWs had much longer durations in MGDSST, resulting in about 5-day biases over the entire domain (Fig. 1h).

Note that we did not find clear dependence on the SST types (i.e., the reference depths) either in MHW metrics or in the errors related to

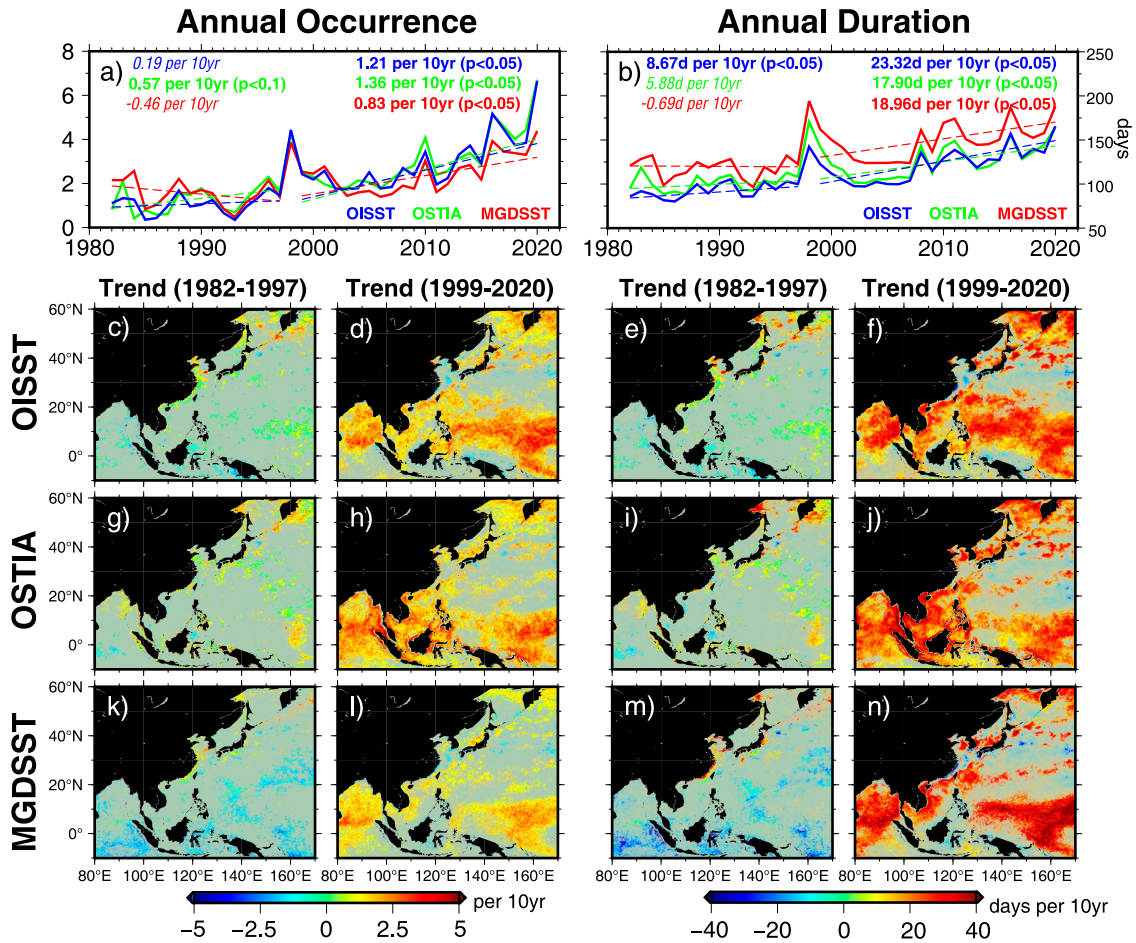

Fig. 2 | Long-term trends of the annual occurrence and durations of MHWs. Time series of the domain-averaged annual (**a**) occurrence and (**b**) duration of MHWs (solid lines) and their linear trends (dotted lines) based on OISST (blue), OSTIA (green), and MGDSST (red) datasets in two periods: 1982−1997 and 1999−2020, together with (**c**−**n**) the spatial distributions of grid-based trends. The linear trends obtained by the Theil-Sen estimator are embedded in (**a**, **b**) (values and dashed lines) with insignificant trends marked by the Italic font, which were based on the annual values. In (**c**−**n**), only significant values ($p < 0.1$) are plotted.

observations (see Supplementary Figs. 5 and 6), and the abovementioned discrepancies will be discussed later.

Long-term variations of MHW activity

After examining the general characteristics of MHWs, we'd like to focus on the temporal variations of MWHs over the AIP region. In addition, by considering the climate regime shift in the late 1990s as mentioned in previous studies[27,44], two separate periods were considered in this study. As shown in Fig. 2a, b, while both occurrence and duration of MHWs reached their highest levels in 1998, distinct differences in their trends were also found before and after 1998. To avoid unexpected under/overestimations, we excluded the year 1998 during the trend estimations. During the early period (1982−1997), MHWs remained few, and the annual durations were also short, having almost no clear trends before 1998. Meanwhile, by considering their spatial distributions, MHWs in the early period were more likely localized phenomena and less organized, while large changes were only seen over some small regions, such as some coastal areas in the East China Sea and the OS (see 1982−1997 panels in Fig. 2).

By contrast, MHW activity was significantly enhanced after 1998, covering large areas over both marginal seas and the open ocean. As a result, more and longer MHWs were observed over most regions in our domain. Results show that the occurrence of MHWs doubled or more during the past two decades (>0.83 per 10 yr), while their durations increased by over 30% (>18.96 d per 10 yr). Interestingly, large increasing trends were seen over almost all the tropical/subtropical and subarctic regions but were limited within a few hot spots in mid-latitudes, such as the Bohai Sea or the southern part of the Sea of Japan.

Although MHW activity obtained by the three datasets varied in a similar way, their differences were not negligible, especially in the estimated long-term trends. For example, during the early period, we did not obtain consistent results using different datasets due to the relatively weak MHW activities, even though the trends were statistically significant in OSTIA and OISST (Fig. 2a). In addition, MGDSST provided some unique patterns with strong descending signals over the tropics and central Pacific regions, which could be barely seen in other datasets (Fig. 2k, m). On the other hand, while the recent enhanced MHW activities were found in all three datasets, the estimated trends varied widely (e.g., Fig. 2b; also see panels for 1999−2020 in Fig. 2).

Uncertainties in regional evaluations

To quantify the extracted MHWs using different datasets and to find which region suffered the most, we introduced an uncertainty index based on the variance of metric differences and used the metrics from OISST as the baselines (Fig. 3; see a global version in Supplementary Fig. 9). It is found that the largest uncertainties are concentrated mainly in tropical regions, especially over the MC covering both marginal seas and open ocean areas. Meanwhile, relatively large uncertainties were also observed in the BOB, the Bohai-Yellow-East China Sea (BS-YS-ECS), and the OS.

To further evaluate the influences of such uncertainties, Fig. 3e−h show the temporal variations of the estimated occurrence and durations of MHWs in four sub-regions. We found that the results in these regions

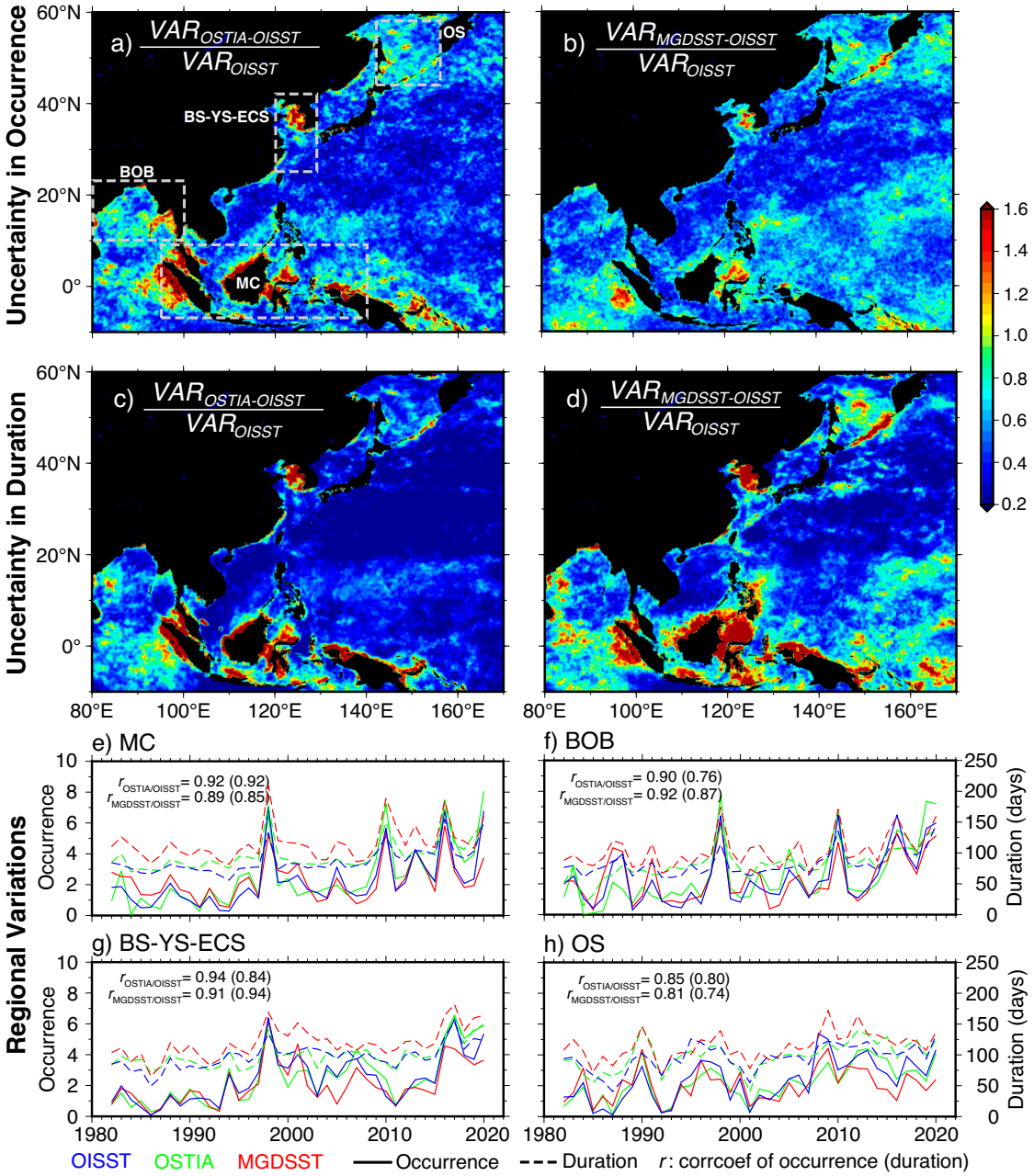

Fig. 3 | Uncertainties in the estimated metrics of MHWs, and time series of area-averaged metrics over four selected regions. a, **c** Uncertainties based on OSTIA and (**b**, **d**) MGDSST datasets, which are defined by the ratios between the variance (VAR) of metric differences and the variance of the baseline from OISST. Temporal variations of area-averaged annual occurrence (solid line) and durations (dashed lines) of MHWs over four selected regions together with the correlation coefficients (*r*): (**e**) the Maritime Continent (MC), (**f**) the Bay of Bengal (BOB), (**g**) the Bohai-Yellow-East China Sea (BS-YS-ECS), and (**h**) the Sea of Okhotsk (OS), which are marked by the boxes in (**a**).

shared similar interannual variations with correlation coefficients over 0.74; however, unlike the results in Fig. 2a, b, they showed non-monotonic biases that varied year to year, leading to the large spread in the estimated linear trends (see Supplementary Table 1).

In addition to the temporal biases, one should also be aware of the differences in their spatial distributions. Figure 4 shows the extracted MHWs in 2020 based on three datasets, and large differences in occurrence and durations among the datasets could easily be seen. It is found that MHWs may exist in one dataset but not in others, or they could be found in totally different areas in a small sub-region. For example, based on OISST, MHWs were detected near the eastern coast of BOB (Fig. 4d), but OSTIA showed they occurred mainly in the western areas (Fig. 4e). Meanwhile, only a few MHWs were detected in OISST and MGDSST within the MC; however, that was not the case in OSTIA which showed much more and longer MHWs, especially near the western coast of Sumatra Island (Fig. 4b, e). Similar to that, MHWs did not even exist near the western coast of the Korean Peninsula in OISST, but the other two datasets showed them. In addition, even for those events that were detected in all datasets, their magnitude could still have a large spread.

One may consider that the regions with large discrepancies may share similar situations or environments; however, our results did not support that. First of all, these regions are located from the tropics to higher latitudes and from coastal areas to the center of open oceans with depths from ~50 m (e.g., the Bohai Sea) to thousands of meters (e.g., the tropical Indian Ocean),

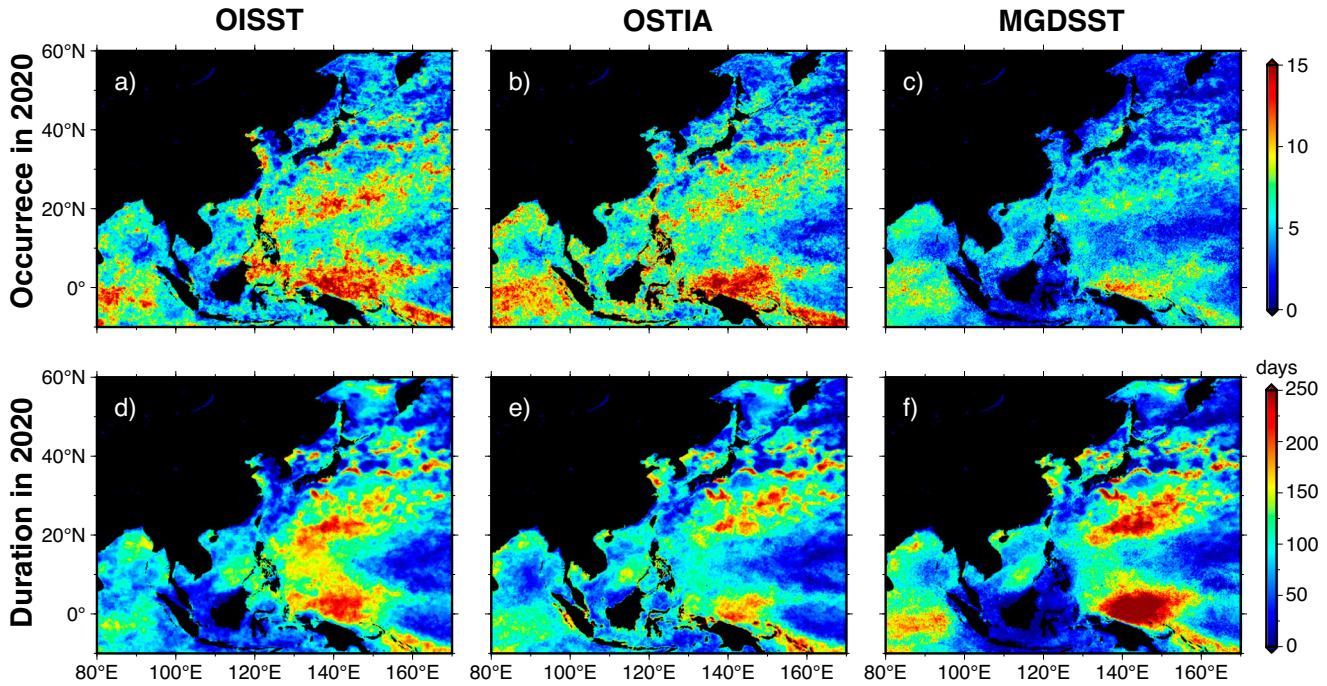

Fig. 4 | MHWs in 2020 based on OISST, OSTIA, and MGDSST. Annual occurrence and durations of MHWs using (**a**, **d**) OISST, (**b**, **e**) OSTIA, and (**c**, **f**) MGDSST.

which are also dominated by different climate and/or weather systems. Meanwhile, their oceanic conditions are also different. Both regions with and without strong ocean currents suffered large uncertainties (e.g., the BOB and the OS), while the mixed layer depths (hence the upper ocean stratification) also varied much among these regions[45], which are believed to be important in MHW formations[46].

Note that the uncertainties mentioned here were designed to represent the spread among the datasets but not to indicate which dataset is better or worse. Similar conclusions could also be obtained by using OSTIA or MGDSST as the baseline (see Supplementary Fig. 3).

Influences of the mean SSTs and their variances

Previous studies suggest that MHWs strongly depend on the mean SSTs and the SST variances[16,18]. Therefore, one may consider the biases and related uncertainties shown above could be attributed to the differences in mean SSTs and their variance among the datasets. To confirm that, we compared three SST datasets and summarized them in Fig. 5. Results indicate that the domain-averaged SSTs and variances of SST anomalies correlated well with the duration (Fig. 2b) and the occurrence (Fig. 2a) of MHWs, respectively (also see Supplementary Fig. 4 for correlation coefficients between SSTs and MHWs). However, as shown in Fig. 5b−g, neither the differences of SSTs nor the variances could explain the distributions of uncertainties found above (Fig. 3a, b), especially for those in tropical regions. For example, although large uncertainties were found in the BOB and the MC, the differences in mean SSTs or variances were quite small. By contrast, the large differences in variance in the Sea of Japan did not lead to large uncertainties. Note that the dot-like patterns in Fig. 5c−g represent the bias-correction in three SST datasets by the Tropical Atmosphere Ocean/Triangle Trans-Ocean buoy Network (TAO/TRITON) Array, which reduced the differences among the datasets; however, our results suggest that such adjustments were limited in about 2-degree area around the buoys and did not reduce the uncertainties in MHW estimations (e.g., Fig. 3a−d).

Possible influences of configurations during the SST analysis

It is known that all three SST datasets ingest in situ observations from ships and buoys, while OISST also started to include the Argo floats in 2016[40]. Therefore, it is not a surprise to see these datasets showing good agreement with each other and having low errors when compared to most in situ data[28,43,47,48] (also see Supplementary Figs. 5, 6, and Supplementary Table 2 for a simple comparison using in situ SST dataset[49]). However, their inputs and related procedures could possibly influence their performance in MHW assessments.

Among the three datasets, OISST only uses the Infra-Red (IR) sensor, while the others combine both IR and microwave (MW) sensors. Although the IR sensors have a better spatial resolution, they also suffer from the influences of cloud cover and weather conditions[50]. With the help of in situ observations, it may not be a large problem; however, as shown in Fig. 1, OISST did exhibit the lowest MHW occurrence in the MC where vigorous convection develops[51]. Similar issues may also influence the uncertainties in coastal regions. When the IR image is not available, the MW sensors cannot obtain high-quality signals near land[52], leading to relatively large errors and hence the discrepancies among the datasets near the coastline[47,53]. On the other hand, although we regridded OSTIA onto a 0.25° mesh, its original high-resolution data could still have some advantages in coastal regions[43] and may result in the relatively higher MHW occurrence there (Fig. 1).

In addition to that, previous studies suggest that the interpolation procedures used for generating satellite SSTs could induce attenuation or spurious small-scale features[54], when a few high-resolution inputs are available. This problem could further induce part of uncertainties by producing spurious MHWs. Meanwhile, MGDSST may suffer more from the smoothing issue, because of its cut-off procedures for high-frequency signals[55,56], which might be the source of its 5-day-longer biases.

Another influence could come from the differences in sea ice treatments. OISST set the SST to −1.8 °C for 100% sea ice concentration (IC), and it also uses a linear ice-to-SST conversion algorithm when IC is larger than 50%[39] (35% in version 2.1 from 2016[40]). Same as OISST, MGDSST also set the SST to −1.8 °C when IC reaches 100%, but no other modification was applied[42]. Unlike the other two datasets, OSTIA uses a NEMOVAR data assimilation scheme[57], which determines the background SST with a 'decay timescale' varying from 5 days to 30 days depending on IC[41]. Therefore, the SSTs over the frequently freezing regions (e.g., the OS) could have great differences among the datasets, leading to large uncertainties in MHW assessments.

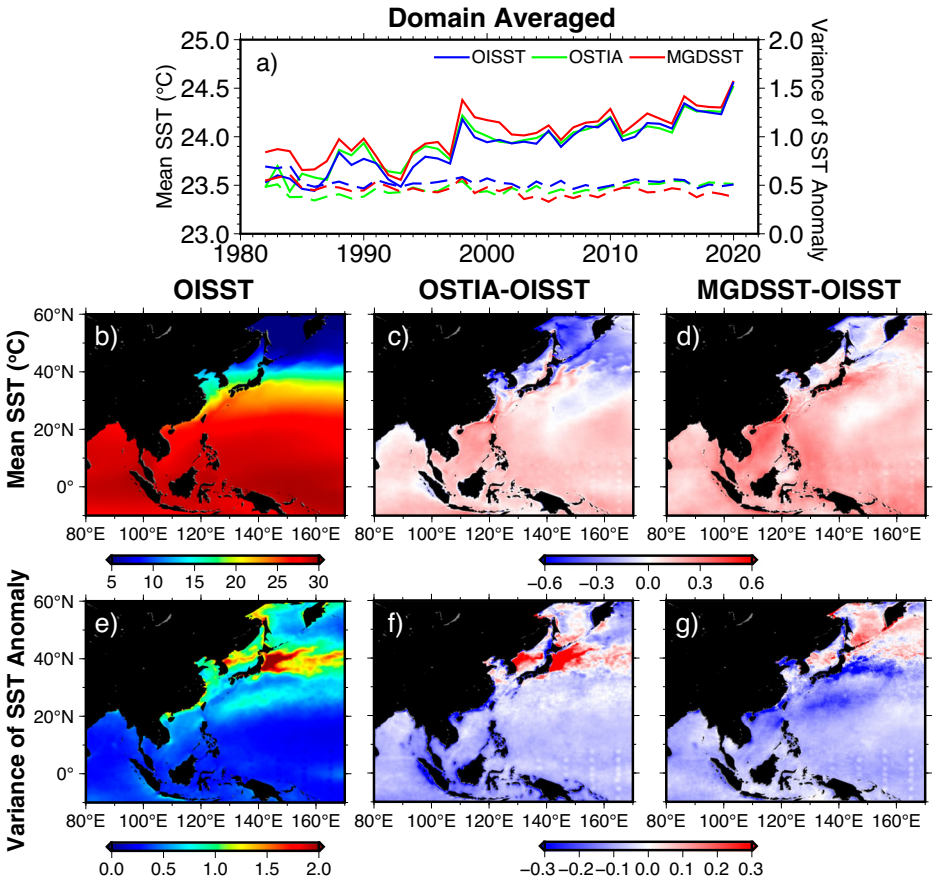

Fig. 5 | Mean SSTs and variances of daily climatology-removed SST anomalies. a Time series of domain averaged SSTs and variances of SST anomalies. **b**–**g** Spatial distributions of mean SSTs and the variances of SST anomalies based on OISST and (**c**, **d**, **f**, and **g**) their differences. Note that panels f-g show the differences of variances, not the variances of differences.

Note that one may consider the multi-product ensemble SST analysis could have better performance in representing SSTs and hence MHWs. However, previous studies suggest that the ensemble median SST does not have to show the lowest errors[28,43]. In addition, our simple three-dataset mean SST also shows similar results and exhibits lower MHW occurrence in the AIP region (see Supplementary Fig. 7), although three datasets are not enough to obtain a robust ensemble mean. Finally, we would like to reiterate that we only tried to assess the uncertainties in MHWs obtained by different datasets but not to provide a quality judgment of them, which should be conducted based on independent in situ data and more proper analyses.

Conclusion

In this study, we analyzed the general characteristics (occurrence and duration) of MHWs over Asia and the Indo-Pacific (AIP) region based on three commonly used SST datasets. In summary, during the last four decades, MHWs tend to occur in the regions near the coastlines and/or with strong warm currents. The occurrence and durations of MHWs were highly correlated, and more frequent MHWs often led to their shorter durations. By contrast, results showed a weak but clear latitude dependence in the mean duration of MHWs, but none was found in their occurrences. In addition, MHWs were rare and inactive before 1998 but were significantly enhanced after 1998 with more and longer MHWs in almost the entire AIP region.

On the other hand, although all SST datasets showed some similar patterns, the large regional differences could not be ignored. Table 1 summarizes the area-averaged MHW metrics (occurrence, duration, and uncertainties) over the AIP region and four subregions mentioned above. Overall, OSTIA showed a 5–10% larger MHW occurrence in most AIP regions, while MGDSST exhibited the lowest, especially in high latitudes. One exception was found in the Maritime Continent, where OISST showed much fewer MHWs. In addition to the occurrence, a large diversity of the locations of MHWs was also found among the datasets. As for MHW duration, a 5-day-longer bias was seen in MGDSST, while the differences between the other two datasets were relatively small. These differences further lead to large uncertainties in MHW metrics and their long-term trends in both coastal and open ocean areas, especially in the Maritime Continent and the East Asia marginal seas; yet no clear dependence was seen in their spatial distributions. Based on an uncertainty index defined by the ratios of variances, discrepancies among the datasets could exceed 0.6 or more. Moreover, although we found that the domain-averaged metrics of MHWs generally followed the mean SSTs and the variances of climatology-removed SST anomalies, neither of them could explain the uncertainties and their distributions. On the other hand, these discrepancies may partially be contributed by sensors, interpolation/smoothing procedures, and sea ice

Table 1 | Mean metrics of MHWs in 1982–2020 over Asia and the Indo-Pacific (AIP) and four selected regions: the Maritime Continent (MC), the Bay of Bengal (BOB), the Bohai-Yellow-East China Sea (BS-YS-ECS), and the Sea of Okhotsk (OS) together with their uncertainties (in brackets), which are defined by the ratios between the variance of metric differences and the variance of the baseline from OISST (see Fig. 3)

Regions	AIP	MC	BOB	BS-YS-ECS	OS
	Occurrence (Uncertainty)				
OISST	87.48 (n/a)	87.46 (n/a)	93.61 (n/a)	95.21 (n/a)	91.35 (n/a)
OSTIA	92.28 (0.65)	97.67 (0.93)	99.45 (0.90)	96.79 (0.85)	86.01 (0.86)
MGDSST	84.65 (0.66)	91.80 (0.76)	93.13 (0.64)	82.00 (0.75)	80.86 (0.90)
Duration (days) (Uncertainty)					
OISST	10.47 (n/a)	9.30 (n/a)	9.93 (n/a)	10.38 (n/a)	11.51 (n/a)
OSTIA	11.43 (0.45)	10.74 (0.85)	10.10 (0.59)	11.12 (0.73)	13.53 (0.55)
MGDSST	16.04 (0.62)	14.55 (1.00)	14.58 (0.66)	17.04 (0.95)	16.59 (0.86)

Table 2 | Descriptive summary of the SST datasets used in this study, where the abbreviations of Infra-Red (IR) and microwave (MW) sensors are listed here: the Advanced Very High Resolution Radiometer (AVHRR), the Visible/Infra-red Imager Radiometer Suite (VIIRS), the Spinning Enhanced Visible Infra-Red Imager (SEVIRI), the Advanced Microwave Scanning Radiometer 2 (AMSR-2), the AMSR-Earth Observing System (AMSR-E), and the Sea and Land Surface Temperature Radiometer (SLSTR)

Dataset	Time Range	Observation input for SST	Type of SST	Resolution	Ice concentration threshold for the SST treatment
OISST[39,40]	1982−2020	IR (AVHRR[a]), in situ (ship/buoy/Argo)	SST at 0.2 m	0.25°	50% (35% from 2016[47])
OSTIA[41]	1982−2020	IR (AVHRR/VIIRS/SLSTR), MW (AMSR2), in situ (ship/buoy)	Foundation SST	0.05° (regridded to 0.25°)	50%
MGDSST[42]	1982−2020	IR (AVHRR/VIIRS/SEVIRI), MW (WindSat/AMSR-2/AMSR-E), in situ (ship/buoy)	SST depth	0.25°	100%

[a]OISST switched to the NOAA Advanced Clear Sky Processor for Ocean (ACSPO) satellite SSTs retrieved from both AVHRR and VIIRS since November 2021[43], but we only used data up to 2020.

treatments in different SST datasets, which greatly influence the small-scall and high-frequency features that are important in MHW assessments. Overall, our study suggests that the use of multiple datasets is crucial for evaluating extreme events.

The discrepancies and spread of datasets are often considered and well-treated in model-based studies[58]; however, they were barely mentioned in the studies using observational datasets, especially the widely-used SSTs. Although previous studies demonstrated the mean state and variations of present SST products are consistent and good for climate studies[28], this may not be true when investigating extreme events. Nowadays, more frequent and longer MHWs are observed not only in Asia and the Indo-Pacific region but also around the global oceans due to the rapidly warming climate[59,60]. Our extended work shows that a large spread in MHW assessments could also be found globally (see Supplementary Figs. 8 and 9), which could further induce large uncertainties in the evaluations and decision-making processes for their impacts on the ecosystem and socio-economy. Although some studies suggest using an ensemble mean of multiple datasets[13], such a process may also lead to the loss of extreme values that are critical in MHW assessments. In addition to that, some recent studies suggest detecting MHWs as spatiotemporally connected pixel-based events[61,62], which could help facilitate the driving mechanisms of MHWs and suppress unexpected spurious events. It could be one possible solution for mitigating some of the discrepancies, but it requires further analyses. More studies also need to be done on this issue, such as more detailed evaluations of SST datasets by independent in-situ observations, investigations on optimal MHW detection algorithms or definitions for different datasets, and the improvement of satellite retrieval algorithms[52].

Method

Data

The daily SST datasets were utilized to diagnose the physical processes of individual MHW events over Asia and the Indo-Pacific regions (80° ~ 170°E, 10°S ~ 60°N). Concerning the different sources and algorithms among different datasets[28], three commonly used global SST analysis datasets that cover the study period of 1982−2020 are selected for comparison, including the National Oceanic and Atmospheric Administration (NOAA) 0.25° daily OISSTv2.1[39,40], the U. K. Met Office 0.05° OSTIA[41], and the 0.25° daily MGDSST[42] from the Japan Meteorological Agency (JMA). In particular, for ease of intercomparison, the 0.05° OSTIA SST was regridded to 0.25° based on the first-order conservative remapping by using the Climate Data Operators software[63]. In addition, the NOAA In situ SST Quality Monitor (iQuam) dataset[49] is also obtained for error estimations in our extra analyses in the Supplementary Information.

All three satellite SST datasets include in situ observations but with different combinations of satellite sensors. OISST uses the Advanced Very High Resolution Radiometer (AVHRR) only during our study period. MGDSST combines both IR and MW sensors, including the AVHRR, the Visible/Infra-red Imager Radiometer Suite (VIIRS), the Spinning Enhanced Visible Infra-Red Imager (SEVIRI), the WindSat, the Advanced Microwave Scanning Radiometer 2 (AMSR-2), and the AMSR-Earth Observing System (AMSR-E). OSTIA uses both IR and MW sensors, including AVHRR, VIIRS, the Sea and Land Surface Temperature Radiometer (SLSTR), and AMSR-2. Despite different observation inputs, these datasets also use different algorithms and thresholds for the areas with ice cover. For ease of comparison, a summary of general information for the three datasets is given in Table 2.

Detection of MHWs

Following previous studies, we defined MHWs as the discrete prolonged anomalously warm events based on the 90th percentile threshold of the climatology-removed SST anomalies from 1982 to 2020[6]. The same period was used for calculating the daily climatology, which is simply defined as the mean SST on a given day of a year computed from the total 39 years. After that, an MHW event is identified when the abnormal warm period lasts over five consequent days or more at each grid point. The same processes were applied to all three datasets using their own thresholds. Note that although no moving window was applied to the 39-year daily climatology, our estimates on MHWs are consistent with previous studies[13,15] and the discrepancies among the three datasets are still clear when using a 31-day moving threshold and 2-gap-day-allowed method[6] (see Supplementary Fig. 1e−g).

After the detection of MHWs, two metrics (occurrence and duration) were estimated for an MHW event at each grid point. In addition, to investigate the long-term variations of MHWs, the monthly metrics were also calculated. Specifically, we calculated the 'monthly occurrence' based on the fractions of their total durations for the long-lasting MHWs that continued over several months[9,64]. For example, the occurrence of a 5-day MHW event from July 30 to August 3 will be counted as 0.4 in July (i.e., two days of its 5-day duration) and 0.6 in August, respectively. Consequently, for simplicity, the monthly duration is obtained by the sum of all MHWs in one month (i.e., MHW days in previous studies[7]), and the annual metrics were the sum of all months in a year. Accordingly, the long-term trends were calculated based on the Theil-Sen estimator using the Python package PyMannKendall[65].

Data availability

The data used in this study are listed as follows: the Optimum Interpolation Sea Surface temperature (OISST; https://psl.noaa.gov/data/gridded/data.noaa.oisst.v2.highres.html), the Daily Sea Surface Temperatures in the Global Ocean (MGDSST; https://www.data.jma.go.jp/gmd/goos/data/pub/JMA-product/mgd_sst_glb_D), the reprocessed foundation SST from the Operational Sea Surface Temperature and Ice Analysis system (OSTIA; https://podaac.jpl.nasa.gov/dataset/OSTIA-UKMO-L4-GLOB-REP-v2.0), and the in situ observational SST from the NOAA In situ SST Quality Monitor (iQuam; https://www.star.nesdis.noaa.gov/socd/sst/iquam).

Code availability

The regridding of OSTIA was performed based on the Climate Data Operators software, which is publicly available at https://code.mpimet.mpg.de/projects/cdo. All analyses were performed using Python. Our codes for

MHW detection are available at https://doi.org/10.5281/zenodo.10475583, and another detection method used for comparison in Supplementary Fig. 1 is obtained from https://github.com/ecjoliver/marineHeatWaves. The PyMannKendall package is publicly available at https://github.com/mmhs013/pymannkendall.

Received: 23 September 2023; Accepted: 3 April 2024;
Published online: 11 April 2024

References

1. Cook, F. et al. Marine heatwaves in shallow coastal ecosystems are coupled with the atmosphere: insights from half a century of daily in situ temperature records. *Front. Clim.* **4**, 1012022 (2022).
2. Pun, I. F., Hsu, H. H., Moon, I. J., Lin, I.-I. & Jeong, J.-Y. Marine heatwave as a supercharger for the strongest typhoon in the East China Sea. *Npj Clim. Atmos. Sci.* **6**, 128 (2023).
3. Smale, D. A. et al. Marine heatwaves threaten global biodiversity and the provision of ecosystem services. *Nat. Clim. Change* **9**, 306–312 (2019).
4. Smith, K. E. et al. Biological Impacts of Marine Heatwaves. *Annu. Rev. Marine Sci.* **15**, 119–145 (2023).
5. Wernberg, T. et al. Climate-driven regime shift of a temperate marine ecosystem. *Science* **353**, 169–172 (2016).
6. Hobday, A. J. et al. A hierarchical approach to defining marine heatwaves. *Progress Oceanogr.* **141**, 227–238 (2016).
7. Frölicher, T. L., Fischer, E. M. & Gruber, N. Marine heatwaves under global warming. *Nature* **560**, 360–364 (2018).
8. Marin, M., Bindoff, N. L., Feng, M. & Phillips, H. E. Slower long-term coastal warming drives dampened trends in coastal marine heatwave exposure. *J. Geophys. Res. Oceans* **126**, e2021JC017930 (2021).
9. Zhang, Y., Du, Y., Feng, M. & Hu, S. Long-lasting marine heatwaves instigated by ocean planetary waves in the tropical Indian Ocean during 2015–2016 and 2019–2020. *Geophys. Res. Lett.* **48**, e2021GL095350 (2021).
10. Benthuysen, J. A., Feng, M. & Zhong, L. Spatial patterns of warming off Western Australia during the 2011 Ningaloo Niño: quantifying impacts of remote and local forcing. *Continental Shelf Res.* **91**, 232–246 (2014).
11. Di Lorenzo, E. & Mantua, N. Multi-year persistence of the 2014/15 North Pacific marine heatwave. *Nat. Clim. Change* **6**, 1042–1047 (2016).
12. Amaya, D. J., Miller, A. J., Xie, S.-P. & Kosaka, Y. Physical drivers of the summer 2019 North Pacific marine heatwave. *Nat. Commun.* **11**, 1903 (2020).
13. Oliver, E. C. J. et al. Longer and more frequent marine heatwaves over the past century. *Nat. Commun.* **9**, 1324 (2018).
14. Marin, M., Feng, M., Phillips, H. E. & Bindoff, N. L. A global, multiproduct analysis of coastal marine heatwaves: distribution, characteristics and long-term trends. *J. Geophys. Res. Oceans* **126**, e2020JC016708 (2021).
15. Holbrook, N. J. et al. A global assessment of marine heatwaves and their drivers. *Nat. Commun.* **10**, 2624 (2019).
16. Oliver, E. C. J. Mean warming not variability drives marine heatwave trends. *Clim. Dyn.* **53**, 1653–1659 (2019).
17. Cheng, Y. et al. A quantitative analysis of marine heatwaves in response to rising sea surface temperature. *Sci. Environ.* **881**, 163396 (2023).
18. Xu, T. et al. An increase in marine heatwaves without significant changes in surface ocean temperature variability. *Nat. Commun.* **13**, 7396 (2022).
19. Ren, X. L., Liu, W., Capotondi, A., Amaya, D. J. & Holbrook, N. J. The pacific decadal oscillation modulated marine heatwaves in the Northeast Pacific during past decades. *Commun. Earth Environ.* **4**, 218 (2023).
20. Gao, G. et al. Drivers of marine heatwaves in the East China Sea and the South Yellow Sea in three consecutive summers during 2016–2018. *J. Geophys. Res. Oceans* **125**, e2020JC016518 (2020).
21. Ren, X. L. & Liu, W. The role of a weakened Atlantic meridional overturning circulation in modulating marine heatwaves in a warming climate. *Geophys. Res. Lett.* **48**, e2021GL095941 (2021).
22. Jacox, M. G. et al. Global seasonal forecasts of marine heatwaves. *Nature* **604**, 486–490 (2022).
23. Liu, J. et al. Robust regional differences in marine heatwaves between transient and stabilization responses at 1.5 °C global warming. *Weather Clim. Extremes* **32**, 100316 (2021).
24. Sen Gupta, A. et al. Drivers and impacts of the most extreme marine heatwave events. *Sci. Rep.* **10**, 19359 (2020).
25. Hayashida, H., Matear, R. J., Strutton, P. G. & Zhang, X. Insights into projected changes in marine heatwaves from a high-resolution ocean circulation model. *Nat. Commun.* **11**, 4352 (2020).
26. Wang, S. et al. Southern hemisphere eastern boundary upwelling systems emerging as future marine heatwave hotspots under greenhouse warming. *Nat. Commun.* **14**, 28 (2023).
27. Lee, S. et al. Rapidly changing East Asian marine heatwaves under a warming climate. *J. Geophys. Res. Oceans* **128**, e2023JC019761 (2023).
28. Yang, C. et al. Sea surface temperature intercomparison in the framework of the copernicus Climate Change Service (C3S). *J. Clim.* **34**, 5257–5283 (2021).
29. Wernberg, T. et al. An extreme climatic event alters marine ecosystem structure in a global biodiversity hotspot. *Nat. Clim. Change* **3**, 78–82 (2013).
30. Teh, L. S. L., Teh, L. C. L. & Rashid Sumaila, U. A Global estimate of the number of coral reef fishers. *PLoS ONE* **8**, e65397 (2013).
31. Holbrook, N. J. et al. Impacts of marine heatwaves on tropical western and central Pacific Island nations and their communities. *Glob. Planet. Change* **208**, 103680 (2022).
32. Wu, L. et al. Enhanced warming over the global subtropical western boundary currents. *Nat. Clim. Change* **2**, 161–166 (2012).
33. Bao, B. & Ren, G. Climatological characteristics and long-term change of SST over the marginal seas of China. *Continental Shelf Res.* **77**, 96–106 (2014).
34. Lee, E.-Y. & Park, K.-A. Change in the recent warming trend of sea surface Temperature in the East Sea (Sea of Japan) over decades (1982–2018). *Remote Sens.* **11**, 2613 (2019).
35. Wang, F. et al. The seas around China in a warming climate. *Nat. Rev. Earth Environ.* **4**, 535–551 (2023).
36. Hu, S. et al. Observed strong subsurface marine heatwaves in the tropical western Pacific Ocean. *Environ. Res. Lett.* **16**, 104024 (2021).
37. Li, Y., Ren, G., Wang, Q. & You, Q. More extreme marine heatwaves in the China Seas during the global warming hiatus. *Environ. Res. Lett.* **14**, 104010 (2019).
38. Wang, D. et al. Characteristics of marine heatwaves in the Japan/East Sea. *Remote Sens.* **14**, 936 (2022).
39. Reynolds, R. W. et al. Daily high-resolution-blended analyses for sea surface temperature. *J. Clim.* **20**, 5473–5496 (2007).
40. Huang, B. et al. Improvements of the Daily Optimum Interpolation Sea Surface Temperature (DOISST) Version 2.1. *J. Clim.* **34**, 2923–2939 (2021).
41. Good, S. et al. The current configuration of the OSTIA system for operational production of foundation sea surface temperature and ice concentration analyses. *Remote Sens.* **12**, 720 (2020).
42. Kurihara, Y., Sakurai, T. & Kuragano, T. Global daily sea surface temperature analysis using data from satellite microwave radiometer, satellite infrared radiometer and in-situ observations (in Japanese). *Weather Service Bull.* **73**, S1–S18 (2006).
43. Huang, B. et al. Understanding differences in sea surface temperature intercomparisons. *J. Atmos. Ocean. Technol.* **40**, 455–473 (2023).

44. Jung, H. K. et al. The influence of climate regime shifts on the marine environment and ecosystems in the East Asian Marginal Seas and their mechanisms. *Deep Sea Res. Part II: Topical Stud. Oceanogr.* **143**, 110–120 (2017).
45. Johnson, G. C. & Lyman, J. M. GOSML: a global ocean surface mixed layer statistical monthly climatology: means, percentiles, skewness, and kurtosis. *J. Geophys. Res. Oceans* **127**, e2021JC018219 (2022).
46. Elzahaby, Y., Schaeffer, A., Roughan, M. & Delaux, S. Why the mixed layer depth matters when diagnosing marine heatwave drivers using a heat budget approach. *Front. Clim.* **4**, 838017 (2022).
47. Woo, H.-J. & Park, K.-A. Inter-comparisons of daily sea surface temperatures and in-situ temperatures in the coastal regions. *Remote Sens.* **12**, 1592 (2020).
48. Hu, Y., Beggs, H. & Wang, X. H. Intercomparison of high-resolution SST climatologies over the Australian region. *J. Geophys. Res. Oceans* **126**, e2021JC017221 (2021).
49. Xu, F. & Ignatov, A. In situ SST Quality Monitor (iQuam). *J. Atmos. Ocean. Technol.* **31**, 164–180 (2014).
50. Petrenko, B., Ignatov, A., Kihai, Y., Stroup, J. & Dash, P. Evaluation and selection of SST regression algorithms for JPSS VIIRS. *J. Geophys. Res. Atmos.* **119**, 4580–4599 (2014).
51. Mao, K. et al. Changes in Global Cloud Cover Based on Remote Sensing Data from 2003 to 2012. *Chinese Geogr. Sci.* **29**, 306–315 (2019).
52. Nielsen-Englyst, P., Høyer, J. L., Alerskans, E., Pedersen, L. T. & Donlon, C. Impact of channel selection on SST retrievals from passive microwave observations. *Remote Sens. Environ.* **254**, 112252 (2021).
53. Vazquez-Cuervo, J. et al. Comparison of GHRSST SST analysis in the Arctic Ocean and Alaskan coastal waters using saildrones. *Remote Sens.* **14**, 692 (2022).
54. Reynolds, R. W. et al. Objective determination of feature resolution in two sea surface temperature analyses. *J. Clim.* **26**, 2514–2533 (2013).
55. Sakurai, T., Kurihara, Y., & Kuragano, T. Merged satellite and in-situ data global daily SST. In *Proc. 2005 IEEE International Geoscience and Remote Sensing Symposium (IGARSS)*, Seoul, Korea, 25–29 July 2005 (2005).
56. Sakurai, T., Kobayashi, H., & Yamane, A. Report to GHRSST XX from JMA. In *Proc. GHRSST XX science team meeting*, Frascati, Italy, 3–7 June 2019 (2019).
57. Fiedler, E. K., Mao, C., Good, S. A., Waters, J. & Martin, M. J. Improvements to feature resolution in the OSTIA sea surface temperature analysis using the NEMOVAR assimilation scheme. *Q. J. R. Meteorol. Soc.* **145**, 3609–3625 (2019).
58. Qiu, Z., Qiao, F., Jang, C. J., Zhang, L. & Song, Z. Evaluation and projection of global marine heatwaves based on CMIP6 models. *Deep Sea Res.Part II* **194**, 104998 (2021).
59. Laufkötter, C., Zscheischler, J. & Frölicher, T. L. High-impact marine heatwaves attributable to human-induced global warming. *Science* **369**, 1621–1625 (2020).
60. Tokarska, K. B. et al. Past warming trend constrains future warming in CMIP6 models. *Sci. Adv.* **6**, eaaz9549 (2020).
61. Bonino, G., Masina, S., Galimberti, G. & Moretti, M. Southern Europe and western Asian marine heatwaves (SEWA-MHWs): a dataset based on macroevents. *Earth Sys. Sci. Data* **15**, 1269–1285 (2023).
62. Sun, D., Jing, Z., Li, F. & Wu, L. Characterizing global marine heatwaves under a spatio-temporal framework. *Progress Oceanogr.* **211**, 102947 (2023).
63. Schulzweida, U. CDO User Guide (2.3.0). *Zenodo* https://zenodo.org/records/10020800 (2023).
64. Oh, H., Kim, G. U., Chu, J. E., Lee, K. & Jeong, J. Y. The record-breaking 2022 long-lasting marine heatwaves in the East China Sea. *Environ. Res. Lett.* **18**, 064015 (2023).
65. Hussain, M. & Mahmud, I. PyMannKendall: a python package for non parametric Mann Kendall family of trend tests. *J. Open Sour. Softw.* **4**, 1556 (2019).

Acknowledgements

N.Z. is supported by his institute (JAMSTEC) through its sponsorship of research activities at the IPRC (JICore) and partially supported by JSPS KAKENHI (20K14560 and 23K11403). X.Z. and Z.D. are supported by the Shanghai International Science and Technology Cooperation Fund Project (23230713800).

Author contributions

N.Z. provided the conception of this study. N.Z. and Z.H. contributed to the design of the study. X.Z. and N.Z. analyzed the SST/MHW data and prepared the first draft of the manuscript. X.Z., N.Z., Z.H. and Z.D. discussed and reviewed the paper before submission.

Competing interests

The authors declare no competing interests.

Additional information

Supplementary information The online version contains supplementary material available at https://doi.org/10.1038/s43247-024-01369-9.

Correspondence and requests for materials should be addressed to Ning Zhao or Zhen Han.

Peer review information *Communications Earth & Environment* thanks Helen Beggs and the other, anonymous, reviewer(s) for their contribution to the peer review of this work. Primary Handling Editors: Olusegun Dada, Heike Langenberg. A peer review file is available.